

Investigation into Use of PMSG-based Wind Farm for Grid Support

Yinan Cui¹, Hasan Shanechi², *Senior Member, IEEE*, Zuyi Li³, *Senior Member, IEEE*, Mohammad Shahidehpour³, *Fellow, IEEE*

Abstract—Reliability and quality of the electrical power supply is of great importance for all grids. A well designed wind farm can help balancing the unpredictable power changes caused by the load-side of the grid. This paper offers some simulation tests on using PMSG-based direct drive wind turbine generator with full scale back-to-back converters for grid support. Different cases have been presented to show that wind energy could be an efficient back-up plan for voltage regulation and a brief study has been carried out which concentrates on possible dynamic compensation on improving the frequency stability of the grid.

Index Terms—dynamic compensation, full scale converters, PMSG, reactive power, short term voltage stability

I. INTRODUCTION

BECAUSE of higher and steadier wind speed, offshore wind turbines could generate more power with more reliability. Lager turbine size, less limits on shipping and erection and the closeness to the coastal centers of the nations, indicate offshore wind farm inevitably will become a vital part of wind energy. EU leads the world's offshore wind power capacity with 2,063 MW installed, and it is expected to reach 40 GW or more by 2020 (EWEA target) [1]. For US, the 420 MW Cape Wind project off the Massachusetts coast has won final approval in April 2010, and there are many projects at different stages of development, including in the Great Lakes [2].

With advances in technology, modern wind turbine generators are capable of responding positively to the network disturbances instead of being unable to respond to the changes in system situation or even aggravating the network's statues. Considering the capability of operation under fault condition and the steadiness of functioning for long-time period, direct-drive wind turbine technology goes ahead of the contest with DFIG. For offshore wind farms, maintenance factor (especially on gearbox part) prevents DFIG to become the first choice. Among the direct-drive wind turbines generators, the one with permanent magnet synchronous generator (PMSG) has become prevalent in the recent years. For PMSG, no additional power supply is needed for the field

excitation and the absence of mechanical components such as slip rings brings higher reliability for generator itself. [3]

To control PMSG at variable speed situation, control of d and q components of the current to control the electromagnetic torque at the generator-side converter and active and reactive power decoupled control at the grid-side converter is proposed [4]. The capability of PMSG-based wind turbine generator to operate uninterruptedly during grid faults, with chopper at DC-link, under different control strategy for converters is tested [5, 6]. Direct-drive wind turbine generator with full scale converters has gained the capability to finish low-voltage ride through process and supply reactive power to the grid [5, 6]. For voltage regulation, a supervisory reactive power control strategy has been proposed on wind-turbine-infinite-bus model [7]. It is found that under this control, both active and reactive power outputs respond very fast in face of solid fault or load changes. However, contribution of the offshore wind farm to voltage and frequency stability of a system other than one connected to infinite bus has not been done yet.

In this paper: system voltage unstable condition cases due to large disturbances (grounded fault) are examined and then the same cases with wind energy support would be studied for comparison. For active power dynamic compensation study, same comparison strategy would be proposed. The simulation tests for all cases in this paper would be implemented with Matlab/Simulink.

II. PMSG-BASED WIND TURBINE GENERATOR WITH FULL SCALE BACK-TO-BACK CONVERTER MODEL AND CONTROL

A. Wind Turbine Model

The input wind power of the wind turbine could be defined as:

$$P_{wind} = \frac{1}{2} \rho A v_{wind}^3 = \frac{1}{2} \rho \pi \left(\frac{D}{2}\right)^2 v_{wind}^3 \quad (1)$$

Where ρ is the air density, A is the blade swept area, D is the blade diameter and v_{wind} is the mean value of measured wind speed.

The mechanical power of the turbine is [8]:

$$P_m = \frac{1}{2} \rho \pi \left(\frac{D}{2}\right)^2 v_{wind}^3 C_p \quad (2)$$

Yinan Cui, Hasan Shanechi, Zuyi Li, and Mohammad Shahidehpour are with the Department of Electrical & Computer Engineering, Illinois Institute of Technology, Chicago, IL 60616 USA (e-mail: ycai3@iit.edu; shanechi@iit.edu; lizu@iit.edu; ms@iit.edu).

Where C_p is turbine efficiency in converting wind energy to mechanical energy.

B. Permanent Magnet Synchronous Generator (PMSG) model

The dynamic model of PMSG in the d-q reference frame is as follows:

$$L_d \frac{d}{dt} i_d = u_d - Ri_d + L_q \omega_e i_q \quad (3)$$

$$L_q \frac{d}{dt} i_q = u_q - Ri_q - L_d \omega_e i_d - \psi \omega_e \quad (4)$$

$$T_e = \frac{1}{2} p [\psi i_q + (L_d - L_q) i_d i_q] \quad (5)$$

Where L_d and L_q are d and q axis inductances, R is resistance of the stator windings, i_d and i_q are d and q axis currents, u_d and u_q are d and q axis voltages, ω_e is electrical rotating angular velocity of the rotor, ψ is the amplitude of the flux induced by the permanent magnets of the rotor in the stator phases, p is number of pole pairs, and T_e is electromagnetic torque [9].

In this dynamics model of PMSG, back electromotive force (back EMF) is assumed to be sinusoidal in the stator. The mechanical system of PMSG can be expressed as:

$$J \frac{d}{dt} \omega_{gen} = T_m - F \omega_{gen} - T_e \quad (6)$$

$$\frac{d\theta}{dt} = \omega_{gen} \quad (7)$$

Where J is the combined inertia of rotor and wind turbine, F is the combined viscous friction of rotor, wind turbine and load, θ is rotor angular position, T_m is the shaft mechanical torque [9].

C. Generator-side Converter Control

Since the PMSG-based wind turbine is equipped with full scale back-to-back converter, ther, the AC power generated by PMSG is converted into DC form through the generator-side converter.

To control stator d-q current components, Constant Torque Angle Control (CTA) is used in this study. CTA keeps the torque angle constant at 90 degrees, causing the stator current vector on q-axis [10]. Therefore, the electromagnetic torque would depend on the magnitude of q-axis current component exclusively. Subsequently, the electromagnetic torque produced by PMSG could be simplified as:

$$T_e = \frac{3}{2} p i_q \quad (8)$$

The current components could be controlled to control the voltage components in (3), (4). This leads to the generator-side converter control strategy with Field Oriented Control (FOC) scheme [10]. The control strategy of generator-side converter is shown in the following figure:

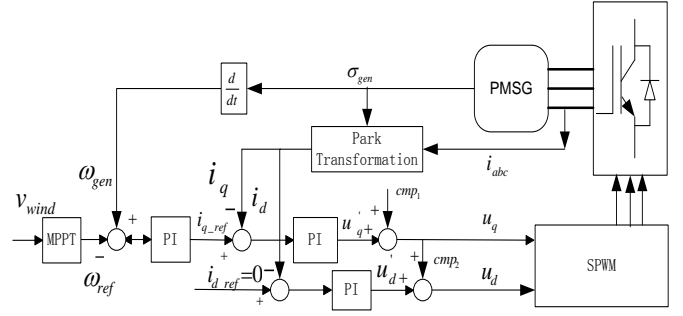


Fig. 1 Generator-side converter control strategy

Where:

$$\begin{aligned} \text{cmp}_1 &= L_d \omega_e i_q + \psi \omega_e + Ri_d \\ \text{cmp}_2 &= -L_q \omega_e i_d + Ri_q \end{aligned} \quad (9)$$

D. Grid-side Converter Control

One objective of controlling of grid-side converter is to keep the DC-link voltage constant regardless of amount of power produced by the generator [11]. The dynamic model of the grid-connected inverter in d-q reference frame rotating at ω_g could be shown to be:

$$\begin{aligned} u_d &= u_{id} - Ri_{id} - L_d \frac{d}{dt} i_d + L \omega_g i_q \\ u_q &= u_{iq} - Ri_{iq} - L_d \frac{d}{dt} i_q - L \omega_g i_d \end{aligned} \quad (10)$$

If the q-axis voltage component could be adjusted to be zero, which is [4]:

$$u_{grid} = u_d + j0 \quad (11)$$

Then, the active and reactive power injected into the network could be represented as:

$$\begin{aligned} P &= \frac{3}{2} u_d i_d \\ Q &= \frac{3}{2} u_d i_q \end{aligned} \quad (12)$$

Therefore, the independent control of active and reactive power could be achieved by controlling the d-q axis current components. The control strategy of grid-side converter is shown as follows:

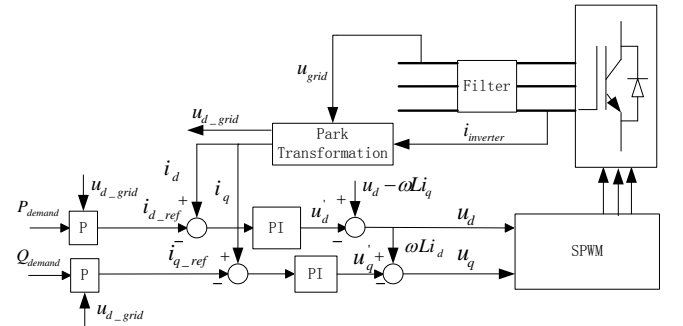


Fig. 2 Grid-side converter control strategy

Where:

$$\begin{aligned} \text{cmp}_1 &= u_d + \omega_g L q^i - R i_d \\ \text{cmp}_2 &= \omega_g L i_q + R i_q \end{aligned} \quad (13)$$

III. SYSTEM DESCRIPTION

The study power system is a 3-generator-8-bus system with offshore wind farm integrated. Total generation capacity for traditional synchronous generators is 426MW, wind farm generation supply is 81MW (wind energy penetration level is around 16% for simulation). Onshore transmission voltage level is 230kV and connection between onshore system and offshore wind farm is HVAC submarine cable operated on the voltage level of 132kV. The receiving end of HVAC submarine cable is bus #8. The load side voltage levels are 10kV and 25kV for constant load (static model) and industrial load.

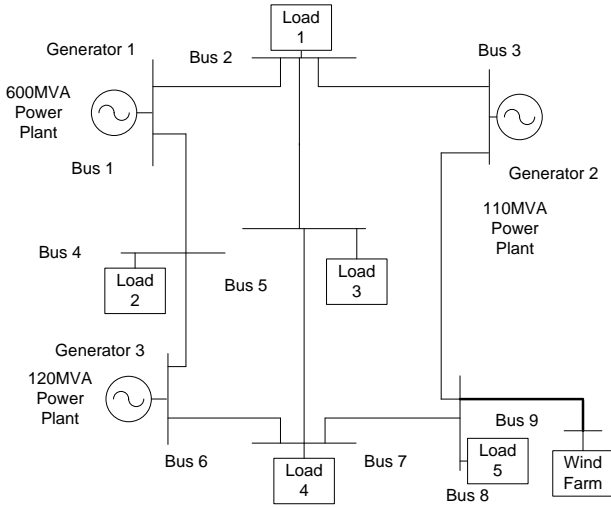


Fig. 3 8-bus system and Wind Farm Integrated into the System with Submarine Cable

IV. SIMULATION RESULTS

To study voltage (reactive power) support capability of the wind farm, a self clearing fault is applied in the system and stability of the system with and without reactive power support from the wind farm is compared. Some of the cases on voltage stability analysis are as follows:

Case 1: Three-phase symmetrical solid fault at bus #7 at $t = 1.5s$ cleared at $t = 1.57s$ ($\Delta t = 0.07s$, 4 cycles). Load center at bus#8.

The load at bus #8 consists of constant PQ load (10MW/10Mvar) and industrial load (modeled as an induction motor with 212MW rated power, voltage stability is load-driven stability based on the published literature [12, 13] and induction motor is widely used as the model of industrial

load for voltage stability studies.), which is about 44% of the total load (507MW). Loads at other buses are only constant PQ load. In this case, the load center (at bus #8) is located very close to the offshore wind farm. For reactive power support, the following control block would be used for grid-side converter.

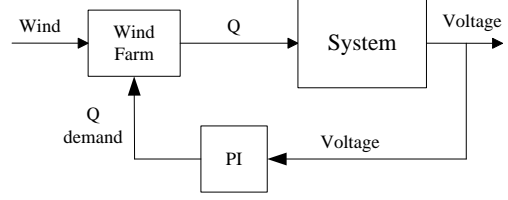


Fig. 4 q-axis current component reference generator of wind farm for voltage regulation

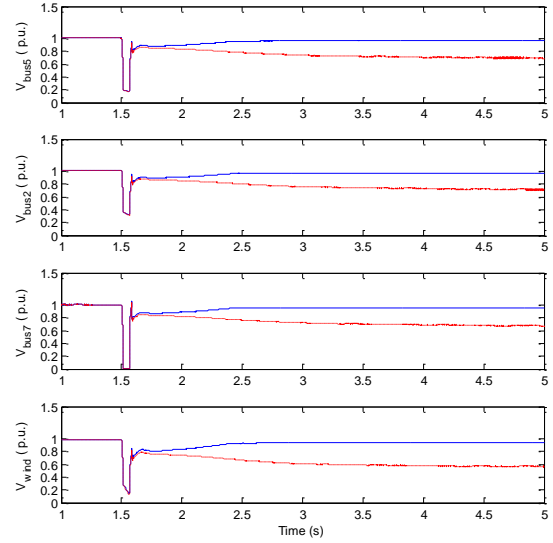


Fig.5 Voltage magnitudes of buses #8, #2, #5 and #7, dotted red lines correspond to no support from the wind farm, blue lines show the improvement due to wind farm support

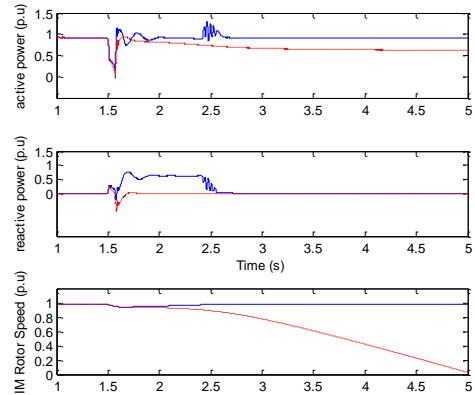


Fig. 6 Power output of wind farm and rotor speed of induction motor at bus #8, dotted red lines correspond to no support from the wind farm, blue lines show the improvement due to wind farm support

This case shows that without wind farm support voltages will not be recovered, whereas with wind farm support they

are recovered in 0.83 seconds. Therefore, wind farm support preserves voltage stability of the network. For wind farm, the reactive power output increased to about 0.6 p.u during the fault, attaining its original values once the voltages recovered. The rotor speed of the induction motor at bus #8 had a slight drop and back to its normal level.

Case 2: Three-phase symmetrical solid fault at bus #7 at $t = 1.5s$ cleared at $t = 1.57s$ ($\Delta t = 0.07s$, 4 cycles). Load center at bus#5.

Bus #5 is relatively far away from wind energy POI. The load at bus #5 consists of constant PQ load (10MW/10Mvar) and industrial load (modeled as an induction motor with 229MW rated power), which is 47% of the total load (507MW).

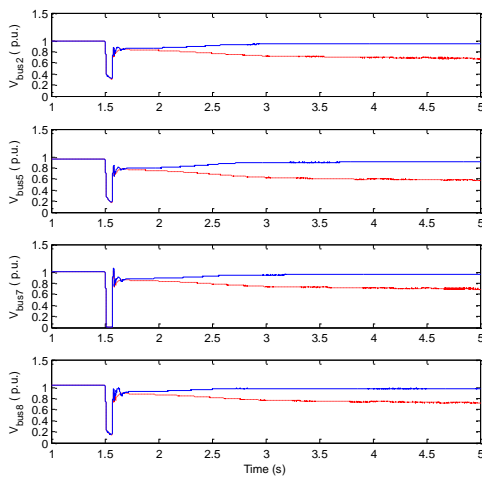


Fig. 8 Voltage magnitudes of buses #2, #5, bus #7 and #8, dotted red lines correspond to no support from the wind farm, blue lines show the improvement due to wind farm support

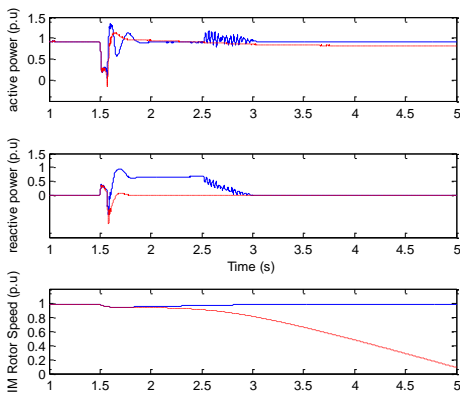


Fig. 7 Power output of wind farm and rotor speed of induction motor at bus #8, dotted red lines correspond to no support from the wind farm, blue lines show the improvement due to wind farm support

It can be seen in this case that voltages will not be recovered without wind farm support, whereas with wind farm support they are recovered in 1.03 seconds. Therefore, wind farm support preserves voltage stability of the network.

For wind farm, the reactive power output increased to about 0.6 p.u during the fault, attaining its original values once the voltages recovered. The rotor speed of the induction motor at bus #5 had a slight drop and back to its normal level.

Case 3: Three-phase symmetrical solid fault at $t = 1.5s$ cleared at bus #7 at $t = 1.58s$ ($\Delta t = 0.08s$, 5 cycles), wind farm would participate in reactive power support when fault happened

The following figures demonstrate the voltage changes for both scenarios where load center located at bus #8 and at bus #5 scenarios.

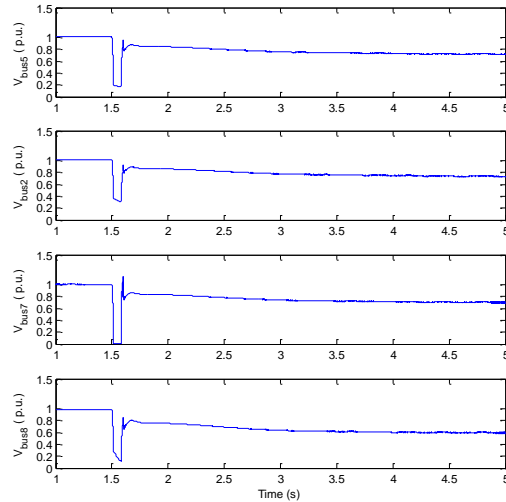


Fig. 9 Voltage magnitudes of buses #2, #5, #7 and #8, load center at bus #8

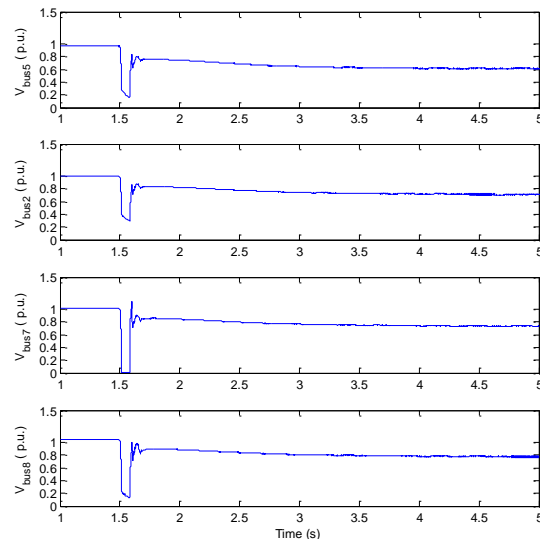


Fig.10 Voltage magnitudes of buses #2, #5, #7 and #8, load center at bus #5

For both scenarios, the voltage magnitudes did not go back to acceptable values even with wind farm support and the system lost its voltage stability.

For dynamic active power compensation study, a large disturbance is introduced into the grid causing large magnitude low frequency oscillation. To mitigate the oscillation, wind farm would adjust its active power output for compensation and the following control scheme would be imposed on grid-side converter control:

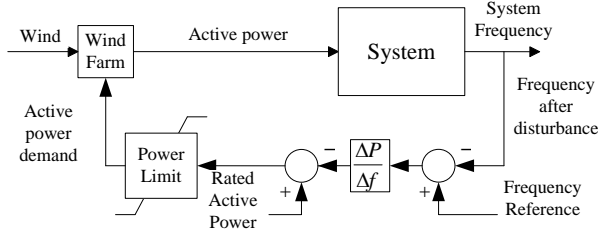


Figure. 11 Active power output control mechanism

Generator #3 would be tripped at $t = 6s$ and remain off line, generator #1 and #2 would pick-up the lost power output.

The results for two cases, with and without wind farm dynamic support are demonstrated as follows:

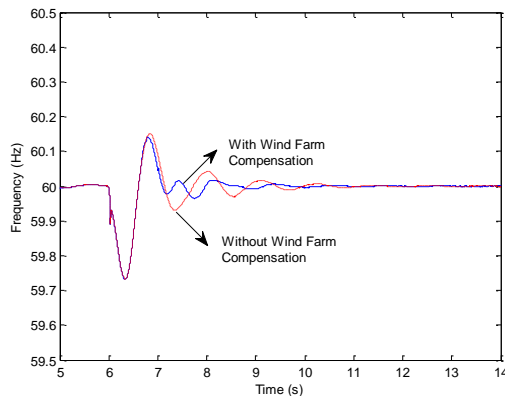


Fig. 12 System frequency after disturbance with and without wind farm compensation

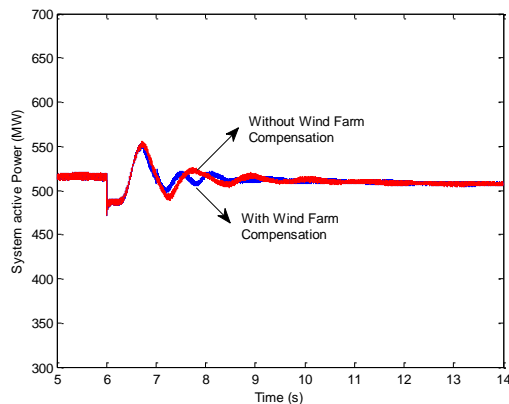


Fig. 13 System Active Power after disturbance with and without wind farm compensation

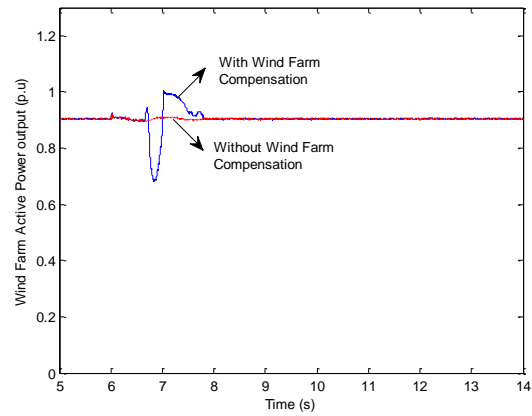


Figure. 14 Wind farm active power output after disturbance with and without wind farm compensation

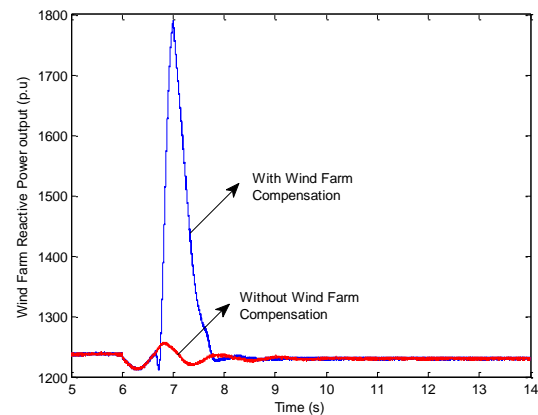


Figure. 15 Wind farm DC-link voltage magnitude after disturbance with and without wind farm compensation

Wind farm active power output is almost constant when it does not participate in dynamic compensation. When wind farm does participate in dynamic compensation, its active power output remains constant for the first half second after the disturbance, as it is producing its maximum power, and then it dips for about half a second due to control action. The energy stored during this time period will peak afterwards. DC-link voltage undergoes a sharp increase due to the reduction of active power output at grid-side and a rapid drop to release the stored energy into the grid.

V. CONCLUSION

According to the simulation results for short-term large-disturbance wind energy grid-support studies, conclusions could be made as followed:

Based on the test cases, wind energy reactive power compensation did make some contributions to grid support on voltage stability improvement. However, reactive power compensation from wind power will not be a vital countermeasure but a back-up plan if large disturbance like solid fault is encountered. The distances between the load center and wind farm would not make a large impact on

voltage stability improvement when large disturbance happens.

With the support from wind farm, oscillation in the system due to large disturbance is mitigated and the system frequency stability is improved. Due to the equipments' physical restriction, the power unbalance condition between DC and AC side of the converters should not last for too long and the power surge at DC side should be limited to a tolerable range. This means active power output reduction at the wind farm is limited.

Fast response of the power electronics in wind turbine generator and flexible control schemes show superiority of wind turbine generator in participating in more system regulations in the future.

VI. REFERENCE

- [1] "Global Wind Energy Council (GWEC) Global Wind 2009 Report." Available at: http://www.gwec.net/fileadmin/documents/Publications/Global_Wind_2007_report/GWEC_Global_Wind_2009_Report_LOWRES_15th.%20Apr..pdf
- [2] "Global Wind Energy Outlook 2010." Available at: <http://www.gwec.net/fileadmin/documents/Publications/GWEO%202010%20final.pdf>
- [3] Li, H. and Chen, Z. "Overview of different wind generator systems and their comparisons." *Renewable Power Generation, IET* 2.2 (2008): 123-38. Print.
- [4] Chinchilla, M., Arnaltes, S., and Burgos, J.C. "Control of permanent-magnet generators applied to variable-speed wind-energy systems connected to the grid." *Energy Conversion, IEEE Transactions* 21.1 (2006): 130-135. Print.
- [5] Anca D. Hansen and Gabriele Michalke. "Modeling and Control of Variable speed Multi-pole Permanent Magnet Synchronous Generator Wind Turbine." *Wind Energy* 11 (2008): 537-554. Print.
- [6] Hansen, A.D. and Michalke, G. "Multi-pole permanent magnet synchronous generator wind turbines' grid support capability in uninterrupted operation during grid faults." *Renewable Power Generation, IET* 3.3 (2008): 333-348. Print.
- [7] Hong-Woo Kima, Sung-Soo Kimb, and Hee-Sang Koa. "Modeling and control of PMSG-based variable-speed wind turbine." *Electric Power Systems Research* 80 (2010): 46-52. Print.
- [8] Fernando D. Bianchi, Hernán De Battista and Ricardo J. Mantz. *Wind Turbine Control Systems-Principles, Modelling and Gain Scheduling Design*. 1st ed. Springer, December 10th, 2010. Print.
- [9] User's Guide (Simulink® Verification and Validation™). Mathworks
- [10] Daryoush Mehrzad, Javier Luque, and Marc Capella. "Vector control of PMSG for wind turbine applications." *Master Thesis, Energy Engineering, M.Sc. (Wind Power Systems, WPS)*, 10, term, 2009. Print.
- [11] R. Peñna, J. C. Clare, and G. M. Asher. "Doubly fed induction generator using back-to-back PWM converters and its application to variable-speed wind-energy generation." *Proc. Inst. Elect. Eng.—Elect. Power* 143.3 (1996): 231-241 Print.
- [12] Thierry Van Cutsem and Costas Vournas. *Voltage Stability of Electric Power Systems*. Springer. 1st ed. Springer, March 31st, 1998. Print.
- [13] Kundur P. *Power System Stability and Control*. EPRI Power System Engineering Series. McGraw Hill, 1994. Print.